ELSEVIER

Journal of Organometallic Chemistry 661 (2002) 169–179

Journal of Organometallic Chemistry

www.elsevier.com/locate/jorganchem

One-electron oxidation of metal enolates and metal phenolates

Michael Schmittel *, Andreas Haeuseler

FB 8-OC 1 (Chemie-Biologie), Universität Siegen, Adolf-Reichwein-Strasse, D-57068 Siegen, Germany

Received 12 April 2002; accepted 26 July 2002

Dedicated to Professor Helmut Werner on the occasion of his retirement in recognition of his tremendous contributions to organometallic chemistry

Abstract

The structure and reactivity of a large number of metal enolates/metal phenolates and their radical cations is analyzed from both a preparative and mechanistic point of view. Special attention is given to the M–O bond cleavage and the C–C coupling on the stage of the radical cations. The insight obtained allowed to devise a novel selective oxidative coupling of enolates and phenolates through an intramolecular variant.

Keywords: Metal enolate; Metal phenolate; Radical cation; Bond cleavage; Stereoselectivity; Kinetics

1. Introduction

Metal enolates C=C–O–M have received extensive attention over the last decades [1] due to the nucleophilicity of the enol subunit and due to the coordination site at the metal that can be used to control chemoselectivity, regioselectivity and stereoselectivity [2]. While metal enolates are often utilized as nucleophiles in aldol reactions and related transformations [2], their umpolung through one-electron oxidation, i.e. the transformation into an electrophilic radical cation, is still widely unexplored. In this personal account we want to summarize our efforts to characterize and to understand the reactivity of different metal enolate radical cations (Ti, Zr, Si and P; P is included though not to be considered a metal).

The motivation to study metal enolate radical cations is based on their electrophilic reactivity which upon proper control should allow to launch stereoselective C–C bond formations either in intermolecular or intramolecular variants. In both modes, the metal has to function as a bridge between the two enolates, but due to the radical cationic character the M–O bond will be drastically weakened in comparison with that in neutral metal enolates. Hence, in order to device oxidative C–C bond formation reactions via metal enolates, the M–O bond cleavage has to be sufficiently slow so that the C–C bond formation process can compete favorably. Otherwise bond formation will occur after M–O bond scission via the α-carbonyl radical in a nonstereoselective manner.

In the first part of this personal account, M–O bond cleavage of the metal enolate radical cations will be described in detail. To allow for the clean characterization of such a process, we have chosen *Fuson*-type [3] metal enolates which carry two bulky mesityl groups in the β-position.

In the second part the intramolecular oxidative coupling reactions of silicon and titanium enolates and phenolates is described. Our concept allows to cross-couple enols in a diastereoselective manner as well as phenol derivatives.

2. Synthesis and structure of the sterically shielded metal enolates

The use of *Fuson*-type metal enolates brings about two major advantages: (i) any nucleophilic attack at the enol radical cation is prevented; and (ii) the dimerization of two enol radical ions is obstructed due to the steric

* Corresponding author. Fax: +49-271-7403270
E-mail address: schmittel@chemie.uni-siegen.de (M. Schmittel).

0022-328X/02/$ - see front matter
PII: S0022-328X(02)01823-5

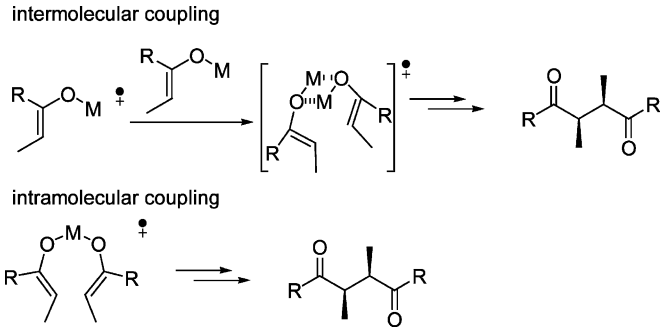

hindrance of the mesityl groups. As a consequence, the M–O bond cleavage is the only observed pathway.

The synthesis of the *Fuson*-type metal enolates **1**–**23** [4–8] was realized through deprotonation of the respective 1-substituted 2,2-dimesitylenol [9] with a base and subsequent in situ reaction with a suitable metal chloride. The yields vary mainly around 40–70%. The somewhat low yields for some examples can be rationalized by a steric congestion due to the mesityl and other bulky groups in systems like **3**, **11** or **21** (Scheme 1).

The steric shielding of the mesityl groups is the reason for a remarkable hydrolytic resistance of the encumbered titanium enolates **7**–**9** [5b]. These compounds survive three months under atmospheric conditions without any significant decomposition, whereas similar uncongested enol derivatives must be stored strictly under inert gas atmosphere. Kinetic investigations by UV and NMR provide for the simple titanium enolate **24** a rate constant for hydrolysis which is 10^3 times higher than that of **9** ($k = 6.4 \times 10\ s^{-1}$ at 32 °C in H_2O–MeCN 1:1).

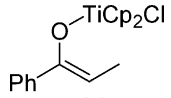

24

According to the structures of **7** [5b], **8** [10], **11** [8], **13** [6], and **19**–**22** [11,12] determined by X-ray crystallography, the mesityl groups always assume a propeller

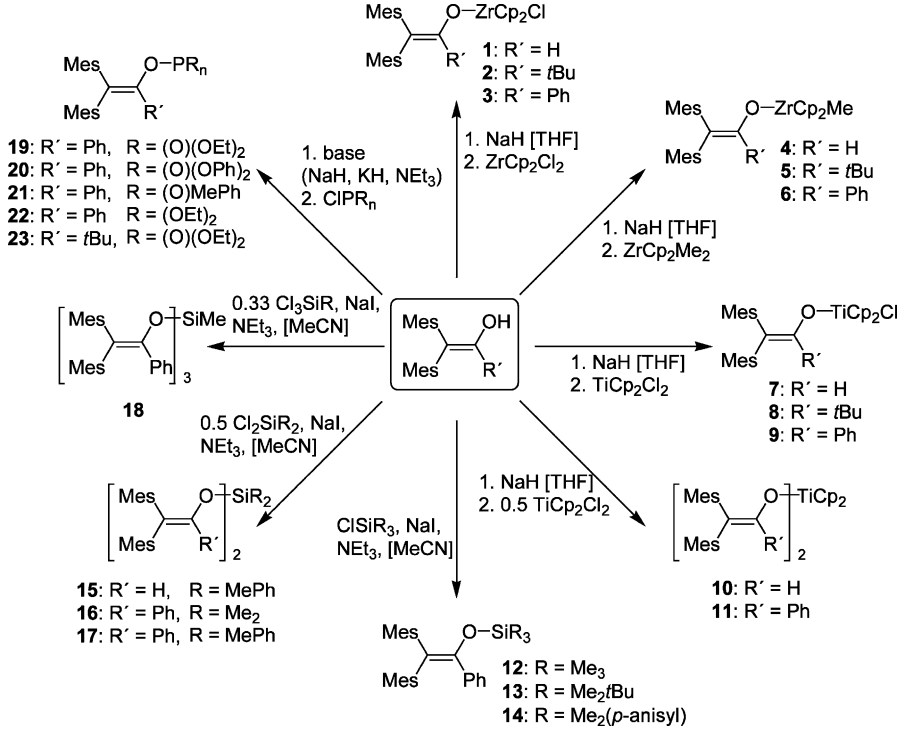

Scheme 1. Synthesis of the sterically shielded enol derivatives **1**–**23** [4–8].

conformation as they cannot arrange coplanar with the double bond. The dihedral angles ϕ_1 and ϕ_2 (C=C–Mes; between the mesityl group and double bond) are placed in a narrow range of 57–66° and 54–60°, respectively. In the phenyl substituted systems **11**, **13** and **19**–**22** all three aryl rings are twisted in the same sense with the smallest dihedral angle between the phenyl ring and the double bond ($\phi_3 = 34$–$45°$). The topology and dynamics of such kind of vinyl polyaryl propellers are intensively investigated by Rappoport [13].

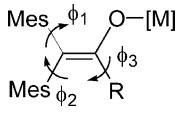

3. Oxidative behavior of the shielded metal enolates

3.1. Cyclic voltammetric investigations

The oxidation potentials of **1**–**23** were first determined by cyclic voltammetry in acetonitrile, but at a scan rate of $v = 100$ mV s^{-1} only irreversible oxidation waves could be obtained. Half-wave potentials $E_{1/2}$ were obtained in dichloromethane–NBu_4PF_6 because of its reduced nucleophilicity. Depending on the metal, the enolate radical cations exhibited reversible waves at scan rates between $v = 0.1$ V s^{-1} (for titanium enolates **8**–**10**) and $v = 1000$ V s^{-1} (for zirconium enolates **1**–**6**). The results are depicted in Table 1.

For further comparison with other enol derivatives we also include the data of the parent enol [14], enol ester [15,16], and the enol ether [17a] to furnish the following ranking:

$$E^{ox}_{1/2}: TiCp_2Cl < ZrCp_2Me < ZrCp_2Cl < H < P(OR)_2 \approx SiR_3 < P(O)(OR)_2 < CONHR < COR < COOR < COCF_3$$

3.2. Reactivity after one-electron oxidation

To elucidate the reactivity of the shielded metal enolate radical cations the course of the follow-up reaction was investigated using EPR measurements, extensive cyclic voltammetric studies and as well as preparative oxidation experiments.

The cyclic voltammograms in acetonitrile are characterized by the irreversible wave of the metal enolate and one additional oxidation wave that was assigned to a substituted benzofuran. The oxidative formation of a benzofuran is already known from the free dimesityl enols [17], and hence an analogous mechanism was postulated [18]. After cleavage of the O–M bond on the stage of the primary metal enolate radical cation an α-carbonyl cation is formed which cyclizes in a *Nazarov*-type reaction. The intermediate undergoes a [1,2]-methyl shift and a final deprotonation leads to the benzofuran product as depicted in Scheme 2.

The key step in product formation is the mesolytic [19] bond cleavage of the primary radical cation that can occur in two different modes (Scheme 3) [20]. The heterolytic mode of O–M bond cleavage would furnish a metal cation M^+ and an α-carbonyl radical, which is further oxidized under the present conditions to the α-carbonyl cation. In the homolytic mode, mesolytic cleavage would lead directly to the α-carbonyl cation.

The mechanistic details of the reactivity of metal enolate radical cations, especially the mode and kinetics of the mesolytic bond cleavage, were analyzed using an arsenal of mechanistic tests: (a) yield of benzofuran in preparative one-electron oxidation experiments; (b)

Table 1
Oxidation potentials of the enol ether derivatives **1**–**23** (V vs. $Fc/Fc^{\bullet+}$) [4–8]

	E_{pa} [a]	$E_{1/2}$ [b]		E_{pa} [a]	$E_{1/2}$ [b]		E_{pa} [a]	$E_{1/2}$ [b]		E_{pa} [a]	$E_{1/2}$ [b]
1	0.45	0.57 [c]	**7**	0.44	0.50 [d]	**13**	0.73	0.67 [d]	**19**	1.01	0.90
2	0.32	0.43 [c]	**8**	0.30	0.26 [e]	**14**	0.68	– [g]	**20**	1.10	0.87
3	0.41	0.44 [c]	**9**	0.38	0.31 [e]	**15**	0.90	0.88 [c]	**21**	0.97	0.86
4	0.51	0.46 [c]	**10**	0.27	0.27 [e]	**16**	0.75	– [g]	**22**	0.74	– [g]
5	0.30	0.35 [c]	**11**	0.27	0.19 [f]	**17**	0.81	0.74 [c]	**23**	1.22	n.d.
6	0.35	0.36 [c]	**12**	0.65	0.69 [c]	**18**	0.79	0.75 [c]			

[a] $v = 100$ mV s^{-1}, in MeCN.
[b] In CH_2Cl_2.
[c] $v = 1000$ V s^{-1}.
[d] $v = 100$ V s^{-1}.
[e] $v = 100$ mV s^{-1}.
[f] 200 V s^{-1}.
[g] Not determinable.

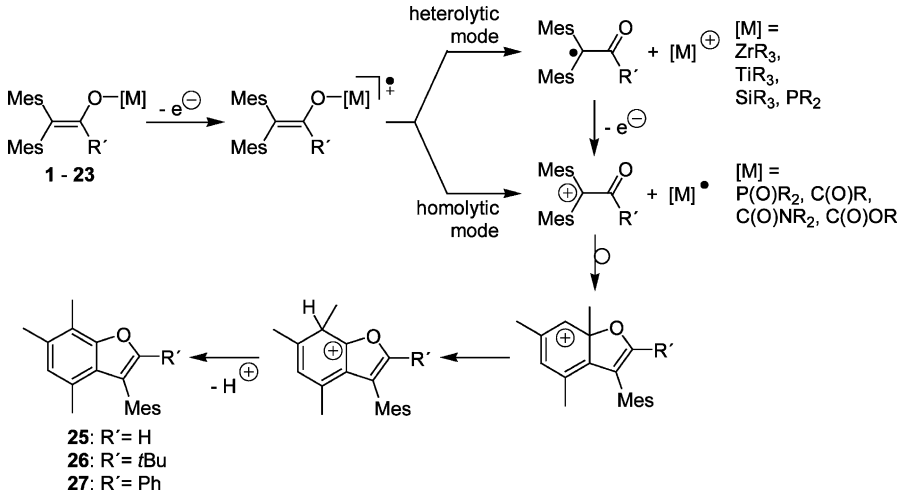

Scheme 2. Mesolytic M–O bond cleavage of the metal enolate radical cations and the follow-up reactions leading to benzofurans **25**–**27**.

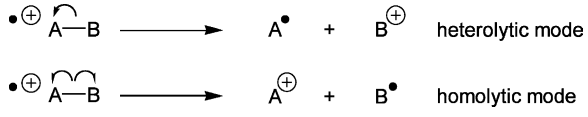

Scheme 3. The homolytic and heterolytic mesolysis of radical cations [19,20]: in this example, A is considered to be the electron-rich part and hence it will act as the electrophore upon oxidation of A–B. Accordingly, in the radical cation of A–B, the charge and spin will reside on A.

kinetic data of the follow-up reaction studying the scan rate dependence of cyclic voltammetric waves; (c) addition of nucleophiles; (d) electron spin resonance spectroscopy (epr); (e) thermochemical cycle calculations; (f) sterically congested titanium and silicon bisenolates were electroanalytically investigated to mimic the unshielded metal bisenolates in the second part of the present paper.

3.2.1. Preparative one-electron oxidation experiments

The metal enolates were oxidized by various oxidants, such as tris(1,10-phenanthroline)iron(III)hexafluorophosphate (**FePhen**), aminium salts or copper(II)triflate in acetonitrile on a preparative scale. In the preponderate number of experiments the benzofurans **25**–**27** could be isolated in good yields (75–95%) with no other side product being found, which underlines the efficiency of the M–O bond cleavage process (Table 2). Only for some phosphoenol derivatives (**19**, **20**, **22**, **23**) the synthesis is less effective. A small turnover of the reaction and the recovery of large amounts of starting material is observed in these cases [7]. This behavior can be explained by the high oxidation potential of the phosphenols (Table 1) and the endothermic reaction enthalpy of electron transfer even for strong oxidants like tris(4-nitrophenyl)aminiumhexachloroantimonate ($E_{1/2} = 1.17$ V_{Fc}).

For the metal bisenolates **10**, **11** and **15**–**17** as well as for the silicon trisenolate **18** all enolate functions were converted into benzofurans when using the appropriate amounts of oxidant, indicated by the good yields.

3.2.2. Kinetics of the cleavage process of the metal enolate radical cations

Knowing that the primary reaction of metal enolate radical cations is M–O bond cleavage allows to determine its kinetics via cyclic voltammetric measurements. All substrates show partial reversible oxidation waves in the accessible scan rate range (up to 20.000 V s^{-1}). From the ratio of the cathodic to the anodic peak

Table 2
Yield of benzofurans **25**–**27** in preparative oxidation experiments [4–8] of **1**–**23** [a]

	Yield (%)	Product		Yield (%)	Product		Yield (%)	Product		Yield (%)	Product
1	95	**25**	**7**	93	**25**	**13**	93	**27**	**19**	41	**27**
2	90	**26**	**8**	95	**26**	**14**	82	**27**	**20**	19	**27**
3	88	**27**	**9**	86	**27**	**15**	69 [b]	**25**	**21**	70	**27**
4	82	**25**	**10**	94 [b]	**25**	**16**	61 [b]	**27**	**22**	46	**27**
5	86	**26**	**11**	88 [b]	**27**	**17**	77 [b]	**27**	**23**	64	**26**
6	80	**27**	**12**	78	**27**	**18**	72 [c]	**27**			

[a] 200 mol% **FePhen**, solvent: CH_3CN.
[b] 400 mol% **FePhen**, Yields refer to all two enolato electrophores.
[c] 600 mol% **FePhen**, Yields refer to all three enolato electrophores.

Table 3
Kinetic data for the cleavage process of the primary radical cations $\mathbf{1}^{\bullet+}$–$\mathbf{23}^{\bullet+}$ [4–8]

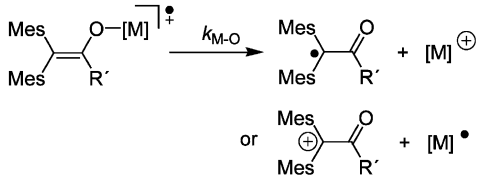

	k_{M-O} [s^{-1}] CH_2Cl_2	k_{M-O} [s^{-1}] CH_3CN		k_{M-O} [s^{-1}] CH_2Cl_2	k_{M-O} [s^{-1}] CH_3CN		k_{M-O} [s^{-1}] CH_2Cl_2	k_{M-O} [s^{-1}] CH_3CN		k_{M-O} [s^{-1}] CH_2Cl_2	k_{M-O} [s^{-1}] CH_3CN
1	–	n.d.	**7**	n.d.	8.5×10^2	**13**	1.3×10^{-1}	6.0×10^2	**19**	3.9×10^{-2}	9.0×10^{-1}
2	3.3×10^2	n.d.	**8**	1.1×10^{-1}	n.d.	**14**	9.4×10^1	$> 10^4$	**20**	5.0×10^{-2}	7.0×10^{-1}
3	3.1×10^2	n.d.	**9**	3.5×10^{-2}	n.d.	**15**	9.0×10^1	–[a]	**21**	5.0×10^{-2}	5.8×10^2
4	8.3×10^2	n.d.	**10**	9.0×10^{-2}	n.d.	**16**	8.0×10^{-1}	–[a]	**22**	1.0×10^4	$> 10^5$
5	5.0×10^2	n.d.	**11**	–	n.d.	**17**	4.0×10^{-1}	–[a]	**23**	0.2×10^0	1.1×10^0
6	–	n.d.	**12**	1.3×10^2	$> 10^4$	**18**	n.d.	n.d.			

[a] Substrate insoluble.

current I_{pc}/I_{pa} the kinetic parameter kt was evaluated according to the method of Nicholson and Shain [21] by applying a mechanism based working curve. The latter was obtained from digital simulation of the cyclic voltammograms assuming an $EC_{irr}E$ mechanism (electron transfer/chemical reaction/electron transfer), as at high scan rates the formation of the benzofuran ring system is too slow to occur on the time scale of the experiment. The kinetic investigation of $\mathbf{1}^{\bullet+}$–$\mathbf{23}^{\bullet+}$ provided first order rate constants for the mesolytic bond cleavage (Table 3).

Remarkably, the rate constants k_{M-O} for the different metal enolate systems differ by six orders of magnitude; e.g. M–O bond cleavage in titanium enol radical cation $\mathbf{9}^{\bullet+}$ ($k_{M-O} = 3.5 \times 10^2\ s^{-1}$) is very slow, while it is very fast in enol phosphite $\mathbf{22}^{\bullet+}$ ($k_{M-O} = 1.0 \times 10^4\ s^{-1}$).

Even in the series of the phosphoenols **19**–**23** rather distinct rate constants were obtained. Table 3 and Fig. 1 show the trend for the rate constants: k_{M-O} (enol phosphate $\mathbf{19}^{\bullet+}$, $\mathbf{20}^{\bullet+}$, $\mathbf{23}^{\bullet+}$) $< k_{M-O}$ (enol phosphinate $\mathbf{21}^{\bullet+}$) $\ll k_{M-O}$ (enol phosphite $\mathbf{22}^{\bullet+}$). Different factors should influence the kinetic results, such as the homolytic bond dissociation energy (BDE) of the M–O bond, the oxidation potential of the metal enolate as well as the steric shielding of the substrates. Semiempirical AM1 calculations indicate that the homolytic bond dissociation energy of the P–O bond is about 20 kcal mol^{-1} smaller for phosphites ($P(OMe)_3$) than that for

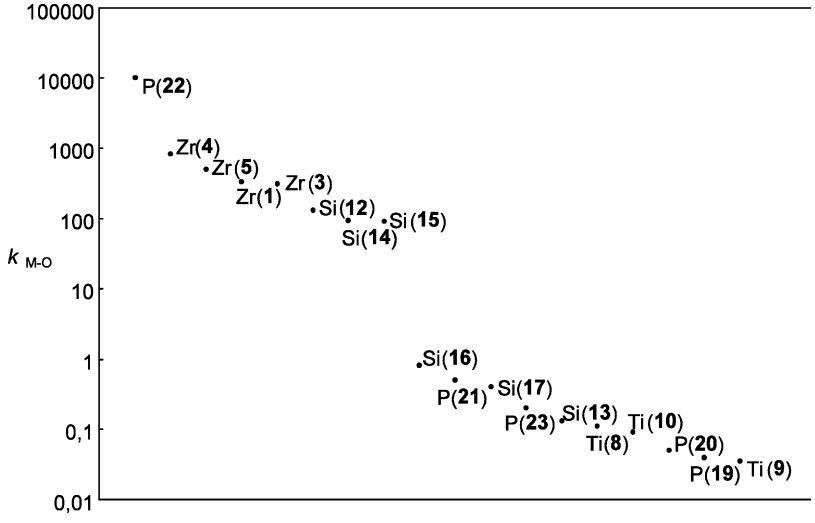

Fig. 1. Graphical presentation of the M–O cleavage rate constants (log k_{M-O} of $\mathbf{1}^{\bullet+}$–$\mathbf{23}^{\bullet+}$).

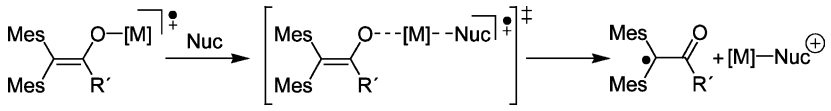

Scheme 4. Nucleophile induced M–O bond cleavage of metal enolate radical cations.

phosphates ($P(O)(OMe)_3$). Taking the different oxidation potentials of the substrates into account, from simple thermochemical cycle calculations one can derive a reduced dissociation energy difference for the radical cations $\mathbf{19}^{\bullet+}$–$\mathbf{20}^{\bullet+}$ versus $\mathbf{22}^{\bullet+}$ of 11 kcal mol^{-1} [7]. This result is in agreement with the kinetic measurements which are illustrated in Fig. 1.

3.2.3. Addition of nucleophiles

The observed dependence of the kinetics on the solvent (dichloromethane vs. acetonitrile in Table 3) already indicates a nucleophilic assistance in the bond cleavage process. To develop a more precise picture of the cleavage mode kinetic investigations on compounds **12**–**14**, **19**–**23** were performed in presence of various oxygen and nitrogen nucleophiles. From silicon and phosphorous it is known that they have the ability of assuming hypervalent structures [22]. In such cases, an attack of nucleophiles may influence the cleavage process of the metal enolate radical cations (Scheme 4).

Indeed, enhanced rate constants of up to 300 s^{-1} for the M–O bond cleavage of silicon enol radical cations $\mathbf{12}^{\bullet+}$–$\mathbf{14}^{\bullet+}$ were observed upon addition of methanol as nucleophile. Additionally, the rate constant of the scission is further increased when a stronger nucleophile (pyridine vs. methanol) or a sterically less hindered nucleophile (2-methylpropan-2-ol vs. methanol) is added [6]. Also, a smaller alkyl group at the silyl moiety (*tert*-butyldimethylsilyl vs. trimethylsilyl) furnishes a faster fragmentation. Such a behavior, which has also been reported in the photoinduced electron transfer (PET) oxidations of benzyltrimethylsilanes [23], α-aminomethylsilanes [24] and simple enol silyl ethers [25], is best rationalized by an associative mechanism as described in Scheme 4. Recent evidence obtained by Dinnocenzo and coworkers indicate that nucleophilic substitution at silane radical cations is concerted as it proceeds with inversion of configuration at silicon [26].

Aside of the silyl enolates only the enol phosphite **22** showed an appreciable dependence of the rate on the addition of nucleophiles. With enol phosphates, enol phosphinates, titanium enolates and zirconium enolates such a behavior was not seen.

3.2.4. Electron paramagnetic resonance

Electron paramagnetic resonance (epr) has been used to characterize the radical cations of enols [27], enol ethers [28] and enol esters [15b]. Epr spectra were measured at low temperature for the metal enolate radical cations of **7** ($g = 2.0043$), **9** ($g = 2.0029$), **19** ($g = 2.0015$), **20** ($g = 2.0012$), and **21** ($g = 2.0019$). In all cases unresolved spectra could be obtained that did not provide any indications about the spin distributions. Nevertheless the data provide ample evidence for the existence of the metal enolate radical cation. Resolved spectra could be obtained for the less shielded titanium enolates **28** and **29** 5c. From the coupling constants and their assignments one can conclude that the spin density is localized on the enol moiety (Fig. 2).

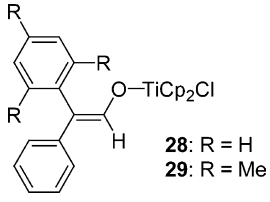

3.2.5. Selectivity of the mesolytic bond cleavage

As already mentioned above M–O bond cleavage is the key step for the sterically encumbered metal enolate radical cations. It can occur in two different modes; a

a^H [G]		
4.82	1 H	C=C–H
3.44	3 H	*o*-/*p*-PhH
1.23	2 H	*m*-PhH
0.84	2 H	*m*-MesH
0.10	9 H	Mes–CH_3

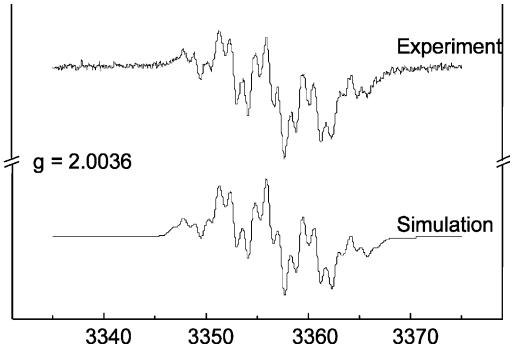

Fig. 2. Epr spectrum of $\mathbf{28}^{\bullet+}$ with its digital simulation [5c].

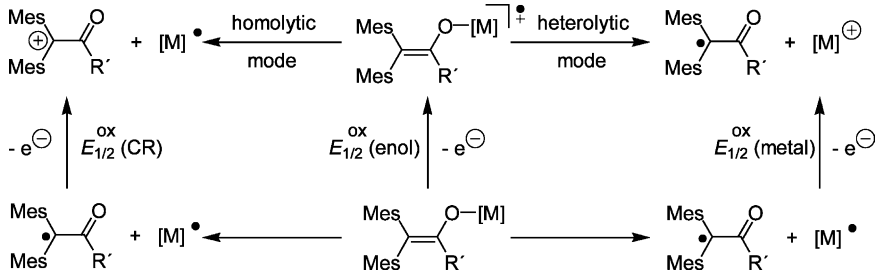

Scheme 5. Thermochemical cycle to distinguish the cleavage mode.

heterolytic and a homolytic mode, respectively [19]. To distinguish the cleavage mode in operation, the amount of electrons consumed at the anode or the amount of oxidant in preparative oxidation experiments does not convey any information, because for both pathways two equivalents of electrons are needed to generate the benzofuran. Therefore, the consideration of a thermochemical cycle like that depicted in Scheme 5 is helpful.

For a prediction of the cleavage mode the oxidation potentials of the different possible cleavage fragments have to be compared as this allows to approximate the thermodynamics of the two modes. For a heterolytic mode the oxidation potential of the metal species $[M]^{\bullet}$ (i.e. $E^{ox}_{1/2}$ (metal)) must be lower than the potential of the α-carbonyl radical ($E^{ox}_{1/2}$ (CR)), whereas for the homolytic fragmentation it has to be vice versa. The values for the α-carbonyl radicals ($E^{ox}_{1/2}$ (CR)) were found to be in the narrow range of $E_{pa} = +0.15 - +0.36$ V_{Fc} [29]. For the zirconium metal fragment, the reduction of the $Cp_2Zr(IV)Me$ cation was determined to $E_{pc} = -1.96$ V_{Fc}. To get similar data for the $Cp_2Zr(III)Cl$ fragment, which is not known yet, a comparison with $Cp_2Zr(IV)Me_2$ ($E_{1/2} = -3.06$ V_{Fc}) and $Cp_2Zr(IV)Cl_2$ ($E_{1/2} = -2.04$ V_{Fc}) helps to estimate the reduction potential of $Cp_2Zr(IV)Cl^+$ to be more cathodic than $E_{pc} \approx -0.9$ V_{Fc}. As a consequence, the oxidation of the Zr(III)-fragment occurs at more cathodic potential than the one of the α-carbonyl radical by more than 1 V. Therefore, zirconocene enolate radical cations follow the heterolytic mesolysis [4]. A similar results was obtained for titanium and silicon enolates **7**–**9** and **12**–**14**, respectively. Also in these cases the oxidation potential of the metal fragment ($Cp_2Ti(III)Cl$ ($E_{pa} = -0.68$ V_{Fc}) [30], '$SiR_3^{\bullet}$' ($E^{ox}_{1/2} = -0.59$ V_{Fc}) [31]) is more cathodic than the one of the α-carbonyl radicals and therefore, a heterolytic mode is reasonable. For phosphoenols the situation is more complicated due to the lack of data for the oxidation of the various phosphorus fragments. Therefore, indirect criteria must be utilized to distinguish between the scission modes. In this context, the consideration of two arguments helps in evaluating the cleavage selectivity: (i) the kinetics of the P–O bond cleavage in presence of nucleophiles; and (ii) the different rate constants in dichloromethane and acetonitrile. The fragmentation of **22** proceeds in a nucleophile assisted manner while for **19**–**21** and **23** no increase of the cleavage rate constant was found in the presence of nucleophiles (cf. part c). Therefore, a heterolytic P–O bond cleavage leading to a α-carbonyl radical and a phosphenium cation is reasonable for $\mathbf{22}^{\bullet+}$ [7]. On the contrary, no influence of the nucleophile concentration on the rate constant is expected when the α-carbonyl cation is a primary product (homolytic mode) which is likely for the radical cations of enol phosphates **19**–**21** and enol phosphinate **23**. Additionally, phosphenium cations are long known as intermediates [32] as well as isolated products [33].

3.2.6. *Sterically shielded metal bisenolates*

To mimic the electronic situation of sterically unencumbered metal bisenolates that should undergo an oxidative coupling to 1,4-diketones (vide infra), we examined the crowded metal bisenolates **10**, **11**, **15**–**17** and also the trisenolate **18**. Interestingly, under oxidative conditions all enolate moieties (two or three) could be converted into benzofurans (Table 2). Two questions arise from this observation: (i) will oxidation of all enolate moieties occur simultaneously or in a stepwise process; and (ii) does the oxidative cyclization occur via an metal enolate radical cation for both or all three enolate electrophores? The first question can be addressed by studying the peak heights I_{pa} of the oxidations waves. It is known from investigations on silicon and titanium monoenolates [5,6] that their oxidation waves accommodate two electrons due to the substrate oxidation and an ensuing oxidation of the intermediate α-carbonyl radical (cf. Scheme 2). By a comparison of the peak heights I_{pa} of the metal bisenolates **10**, **15**, **17** and **18** [8] with the ones of the silicon and titanium monoenolates **12** and **7**, respectively, it could be concluded that also for the bisenolates the initial oxidation wave contains two electrons in case of an irreversible cyclic voltammogram, whereas a single electron is transferred in the reversible oxidation at higher scan rates ($v = 1000$ V s^{-1}) (Table 4).

Beside the reversible wave a second, irreversible oxidation wave is observed about 300 mV shifted anodically in the cyclic voltammograms of silicon bisenolates **15**–**17**. This wave can be assigned to the oxidation of the radical cation to the dication [8]. This

Table 4
Comparison of relative peak heights I_{pa} of mono- and bisenolate systems [8]

12 [a]	**15** [a]	**17** [a]	**17** [b]	**18** [b]	**7** [b]	**10** [b]
$I_{pa} \equiv 2.00$	$I_{pa} = 2.85$	$I_{pa} = 2.01$	$I_{pa} = 1.20$	$I_{pa} = 0.97$	$I_{pa} \equiv 1.00$	$I_{pa} = 1.19$

[a] Irreversible oxidation wave in MeCN at $v = 100$ mV s^{-1}.
[b] Reversible oxidation wave in CH_2Cl_2 at $v = 1000$ V s^{-1}.

observation discloses that only one enolate electrophore is oxidized in the first step and that the transformation of several enolate moieties to the corresponding benzofurans will occur in a stepwise process.

The elaboration of the second question concerning the mechanistic pathway of the benzofuran formations is best addressed in two distinct steps: (i) oxidative cyclization of the first enolate fragment; and (ii) the reactivity of all further enolate moieties in the course of reaction. It is most reasonable to assume that the first enolate in silicon and titanium bis- and trisenolates reacts in a similar manner as in metal monoenolates and that the M–O bond is cleaved on stage of the radical cation (metal bisenolate radical cations are detected in fast-scan cyclic voltammetry) in a heterolytic mesolysis. This scenario is supported by the fact that for **10** and **11** the α-carbonyl radical could be detected in cyclic voltammetric measurements as the primary cleavage product [8].

Several mechanistic alternatives have to be considered for the fate of the resultant metal(IV)monoenolate cations that are formed after the mesolytic cleavage. (i) Further oxidation of the cation and a subsequent second M–O bond cleavage process; (ii) reaction of the cation with a nucleophile leading to an enolate derivative with an even lower oxidation potential which is then oxidized as in (*a*); (iii) acid liberated in the oxidative benzofuran formation hydrolyzes part of the metal bisenolates, thereby setting free the enols that are oxidized to the benzofurans. The latter mechanism should be dominant in the absence of base whereas the observation of the α-carbonyl radical in the cv of **10** and **11** argues for route (i) if a base is present.

4. Oxidative coupling of metal bisenolates–biphenolates

4.1. Silicon and titanium bisenolates

The oxidative coupling of enol derivatives [34] has been established as a valuable route for the synthesis of 1,4-dicarbonyl compounds [35,36]. Unfortunately, it suffers from some severe limitations, such as lacking options for the cross-coupling [37] of different enol compounds or lacking control over the stereoselectivity. Both problems could only be solved for specific systems [37,38]. To open up a more general reaction concept, we investigated the oxidative intramolecular C–C coupling of metal bisenolates on the stage of the radical cation. Obviously, a selective coupling of different enol compounds should now become possible when starting from unsymmetric metal enolates (Scheme 6). As can be seen in the following, the intramolecular reaction also furnishes the product in a highly diastereoselective manner.

To select a promising metal for the metal bisenolates, several considerations have to be taken into account, such as low oxidation potential (Table 1), slow M–O bond cleavage rates (Table 3) and synthetic availability. From our investigations the metals titanium and silicon should offer the best chances, and as a consequence the titanium and silicon bisenolates of propiophenone and acetophenone **30**–**35** and silicon trisenolate **36** were chosen as model compounds (Table 5).

The preparation of the symmetric metal polyenolates **30**–**35** and **36** was realized by the reaction of the lithium enolate with dichlorosilane and dichlorotitanocene, respectively. [39] The unsymmetric silicon bisenolates **34** and **35** were synthesized according to a method described by Rathke via an aminosilane intermediate [40]. The various metal bisenolates were then oxidized on a preparative scale by one-electron oxidants such as Fe(III), Ce(IV) or Cu(II) ions to afford 1,4-diketones as coupling products. The results are summarized in Table 5.

The oxidation of the different silicon bisenolates furnishes the corresponding 1,4-diketones as coupling products in moderate yields (36–59%) and in good *d*,*l*-diastereoselectivities (*de* ≈ 80%). For the analogous

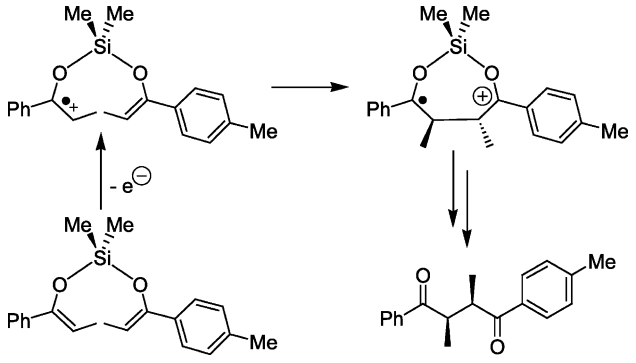

Scheme 6. Concept of the intramolecular oxidative coupling reaction of metal enolates.

Table 5
Preparative one-electron oxidations with silicon and titanium bisenolates [39a]

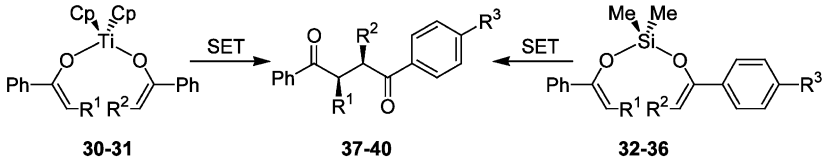

30-31 37-40 32-36

	Entry	Bisenolate	R^1	R^2	R^3	Oxidant	Product (% yield)	de[d] (%)
Ti	1	**30**	Me	Me	–	**FePhen**	**37** (39)	0
	2	**30**	Me	Me	–	$Cu(OTf)_2$	**37** (23)	0
	3	**31**	H	H	–	**FePhen**	**38** (17)	–
	4	**30**+**31**				**FePhen**	**37**+**38**+**40**[c]	–
Si	5	**32**	Me	Me	H	**FePhen**[a]	**37** (57)	82
	6	**32**	Me	Me	H	CAN[b]	**37** (59)	80
	7	**33**	H	H	H	$Cu(OTf)_2$	**38** (48)	–
	8	**32**+**33**				$Cu(OTf)_2$	**37** (50)+**38** (30)	–
	9	**34**	Me	Me	Me	CAN	**39** (66)	78
	10	**35**	Me	H	H	CAN	**40** (36)	–
	11	Trisenolate **36**	Me	Me	H	CAN	**37** (60)	97

[a] **FePhen**: $[Fe(phen)_3](PF_6)_3$.
[b] CAN: $[Ce(NH_4)_2](NO_3)_6$.
[c] Ratio of products **37**:**38**:**40** = 2.8:0.1:1.0.
[d] *d,l* diastereomer is favored over the *meso* diastereomer.

titanium derivatives the obtained yield was remarkably lower (17–39%) and importantly no diastereoselectivity was observed in the coupling reaction of **30** (Table 5, entries 1 and 2). From the results it is obvious that the concept of the intramolecular oxidative coupling of enolates was successful only for the silicon derivatives as demonstrated by the cross experiment (Table 5, entry 8) and the selective synthesis of the unsymmetric 1,4-diketones starting from **34** and **35**, respectively (Table 5, entries 9 and 10). The concept failed in case of the titanium enolates, because a cross experiment with a mixture of **30** and **31** furnished not only the symmetric coupling products **37** and **38** but also the unsymmetric 1,4-diketone **40**. Formation of the latter product can only be rationalized by an intermolecular process. Experimental evidence indicates clearly that the intermolecular coupling occurs via the titanium radical cations and not via α-carbonyl radicals after Ti–O bond cleavage.

The *d,l* diastereoselectivity in the coupling of silicon bisenolates **32** and **34** can be explained along the following considerations. As deduced from investigations on the sterically shielded metal enolates, any carbon–carbon bond formation will occur on stage of the radical cation. Hence, the diastereoselectivity will be determined by the energy difference in the transition states of the two diastereomorphic approaches (Scheme 7). The steric interactions between the phenyl and the methyl group are smaller for the *lk* approach than for an *ul* approach. Thus, the preferred formation of the *d,l* diastereoisomers is evident. The steric influence of the spectator groups R^1 and R^2 on the diastereoselectivity can be additionally visualized by the trisenolate **36**. The preparative oxidation furnished *d,l* isomer of 1,4-diketone **37** in 60% yield and with a high selectivity of *de* = 97% (Table 5, entry 11).

One question remains from the above investigations on the intramolecular oxidative coupling of metal bisenolates: why does our concept fail for the intramolecular coupling of titanium derivatives? Why is intermolecular more rapid than intramolecular C–C bond formation? When we compare the metals Si and Ti we realize that the O–M–O bond angle differs for silicon and titanium bisenolates. Whereas for silicon [39a] the angle is about 107–109°, it is smaller for titanium [41] by

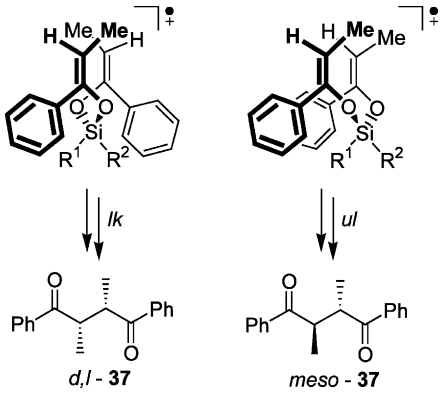

Scheme 7. Model for the different transition states in the intramolecular, oxidative coupling of silicon bisenolates.

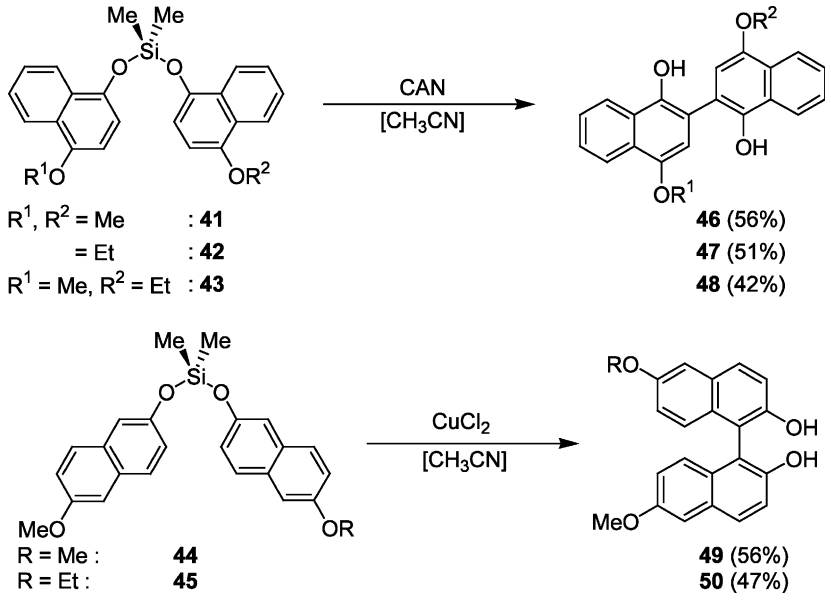

Scheme 8. Oxidative coupling of silicon bisnaphtholates [43].

about 15° (90–95°). As seven-membered transition states are more strained when they have one small angle (90–95°) in the ring, we assume that due to this strain the cyclization step in titanium bisenolate radical cations is slower than intermolecular coupling.

4.2. Silicon binaphthols

To further extent the concept, we investigated whether electron-rich phenolic groups would equally undergo an analogous intramolecular oxidative coupling thus opening an synthetically valuable route to biphenols. Due to the intramolecularity a selective cross-coupling of different starting compounds should become possible, and moreover, the carbon–carbon bond formation should occur in an *ortho* selective manner. Such route may serve as a helpful synthetic alternative in the cross-coupling of natural naphthols that are intensively investigated by Bringmann et al [42].

The symmetric and unsymmetric silicon binaphtholates **41**–**45** were synthesized analogously to the corresponding bisenolates. After reaction with different one-electron oxidants the binaphthols **46**–**50** were obtained in 42–56% yield (Scheme 8) [43].

The intramolecular nature of the oxidative C–C coupling was demonstrated by the formation of the unsymmetric binaphthols **48** and **50**. While **50** was formed without a trace of the symmetric binaphthols (that could potentially form in intermolecular reactions), the formation of **48** was accompanied by small amounts (5%) of the symmetric products **46** and **47**. Another control experiment, oxidation of a 1:1 mixture of **41** and **42**, only provided binaphthols **46** and **47**. Recapitulating, the oxidative coupling in silicon binaphtholates appears to proceed via an intramolecular route; small amounts of intermolecularly derived products therefore are most likely due to hydrolysis of the reactants in the latter stage of the reaction (when large amounts of protons have been liberated) and oxidative coupling of free naphthols.

5. Summary

In summary, we have been able to prepare a large number of metal enolates and to investigate their radical cation reactivity from both a preparative and mechanistic point of view. The insight obtained allowed to devise a novel selective oxidative coupling of enolates and phenolates through an intramolecular variant. Future will show whether these couplings can be used for enantioselective processes by attaching chiral ligands to the metal centers.

Acknowledgements

We are indebted to the Deutsche Forschungsgemeinschaft (SFB 347) and to the Fonds der Chemischen Industrie for generous support.

References

[1] (a) D.A. Evans, L.R. McGee, J. Am. Chem. Soc. 103 (1981) 2876;
(b) C.F. Longmire, S.A. Evans, Jr., J. Chem. Soc. Chem. Commun. (1990) 922;
(c) D.A. Evans, D.L. Rieger, M.T. Bilodeau, F. Urpi, J. Am. Chem. Soc. 113 (1991) 1047;
(d) W.R. Roush, J. Org. Chem. 56 (1991) 4151;
(e) Y. Xiang, E. Olivier, N. Ouimet, Tetrahedron Lett. 33 (1992)

457;
(f) K. Miura, T. Nakagawa, S. Suda, A. Hosomi, Chem. Lett. (2000) 150.
[2] R.E. Gawley, J. Aubé, Principles of Asymmetric Synthesis (Chapters 3–5), Pergamon, Oxford, 1996, p. 35.
[3] R.C. Fuson, D.H. Chadwick, M.L. Ward, J. Am. Chem. Soc. 68 (1946) 389.
[4] Zirconium enolates: (a) M. Schmittel, R. Söllner, J. Chem. Soc. Chem. Commun. (1998) 565;
(b) M. Schmittel, R. Söllner, J. Chem. Soc. Perkin Trans. 2 (1999) 515.
[5] Titanium enolates: (a) M. Schmittel, R. Söllner, Angew. Chem. Int. Ed. Engl. 35 (1996) 2107;
(b) M. Schmittel, H. Werner, O. Gevert, R. Söllner, Chem. Ber. Recl. 130 (1997) 195;
(c) M. Schmittel, R. Söllner, Chem. Ber. Recl. 130 (1997) 771.
[6] Silicon enolates M. Schmittel, M. Keller, A. Burghart, J. Chem. Soc. Perkin Trans. 2 (1995) 2327.
[7] Enol phosphates: (a) M. Schmittel, J.P. Steffen, A. Burghart, J. Chem Soc. Chem. Commun. (1996) 2349;
(b) M. Schmittel, J. P. Steffen, A. Burghart, Acta Chem. Scand. 53 (1999) 781.
[8] Polyenolates **10**,**11**, **15**–**18**: M. Schmittel, A. Burghart, H. Werner, M. Laubender, R. Söllner, J. Org. Chem. 64 (1999) 3077.
[9] Synthesis: (a) (R = H) S.E. Biali, Z. Rappoport, J. Am. Chem. Soc. 106 (1984) 5641;
(b) (R = tBu) D.A. Nugiel, Z. Rappoport, J. Am. Chem. Soc. 107 (1985) 3669;
(c) (R = Ph) E.B. Nadler, Z. Rappoport, J. Am. Chem. Soc. 109 (1987) 2112.
[10] H. Werner, M. Laubender, M. Schmittel, R. Söllner, Z. Krist. New Cryst. Struct. 214 (1999) 47.
[11] A. Burghart, M. Schmittel, M. Keller, J. Chem. Crystallogr. 29 (1999) 421.
[12] A. Burghart, PhD thesis, Würzburg, 1997.
[13] (a) M. Schmittel, M. Keller, A. Burghart, Z. Rappoport, A. Langels, J. Chem. Soc. Perkin Trans. 2 (1998) 869;
(b) Z. Rappoport, S.E. Biali, Acc. Chem. Res. 30 (1997) 307.
[14] M. Röck, M. Schmittel, J. Prakt. Chem. 336 (1994) 325.
[15] (a) M. Schmittel, J. Heinze, H. Trenkle, J. Org. Chem. 60 (1995) 2726;
(b) M. Schmittel, K. Peters, E.-M. Peters, A. Haeuseler, H. Trenkle, J. Org. Chem. 66 (2001) 3265.
[16] M. Schmittel, H. Trenkle, J. Chem. Soc. Perkin Trans. 2 (1996) 2401.
[17] (a) M. Schmittel, M. Röck, Chem. Ber. 125 (1992) 1611;
(b) M. Schmittel, Top. Curr. Chem. 169 (1994) 183.
[18] A mechanism involving cyclization on the stage of the metal enolate radical cation prior to M–O bond cleavage can be excluded due to the steric repulsion of the *ortho* methyl groups and the ligands at the metal.
[19] The expression *mesolytic* has been coined by Maslak [20] for the bond scission of radical ions; one distinguishes the heterolytic and the homolytic mode.
[20] P. Maslak, J.N. Narvaez, Angew. Chem. Int. Ed. Engl. 29 (1990) 283.
[21] R.S. Nicholson, I. Shain, Anal. Chem. 36 (1964) 706.
[22] R.J.P. Corriu, J.C. Young, in: S. Patai, Z. Rappoport (Eds.), The Chemistry of Organic Silicon Compounds, Wiley, New York, 1989, p. 1241.
[23] (a) J.P. Dinnocenzo, S. Farid, J.L. Goodman, I.R. Gould, W.P. Todd, S.L. Mattes, J. Am. Chem. Soc. 111 (1989) 8973;
(b) J.P. Dinnocenzo, S. Farid, J.L. Goodman, I.R. Gould, W.P. Todd, Mol. Cryst. Liq. Cryst. 194 (1991) 151;
(c) K.P. Dockery, J.P. Dinnocenzo, S. Farid, J.L. Goodman, I.R. Gould, W.P. Todd, J. Am. Chem. Soc. 119 (1997) 1876.
[24] X.M. Zhang, S.R. Yeh, S. Hong, M. Freccero, A. Albini, D.E. Falvey, P.S. Mariano, J. Am. Chem. Soc. 116 (1994) 4211.
[25] T.M. Bockman, J.K. Kochi, J. Chem. Soc. Perkin Trans. 2 (1996) 1633.
[26] H.J.P. de Lijser, D.W. Snelgrove, J.P. Dinnocenzo, J. Am. Chem. Soc. 123 (2001) 9698.
[27] M. Schmittel, G. Gescheidt, M. Röck, Angew. Chem. Int. Ed. Engl. 33 (1994) 1961.
[28] (a) G. Behrens, E. Bothe, G. Koltzenburg, D. Schulte-Frohlinde, J. Chem. Soc. Perkin Trans. 2 (1980) 883;
(b) M.C.R. Symons, B.W. Wren, J. Chem. Soc. Perkin Trans. 2 (1984) 511.
[29] M. Röck, M. Schmittel, J. Chem. Soc. Chem. Commun. (1993) 1739.
[30] S.V. Kukharenko, G.L. Solveichik, V.V. Strelets, Bull. Acad. Sci. USSR Div. Chem. Sci. (Engl. Transl. 35 (1986) 926.
[31] The reduction potential of trimethyl silyl cation determined in acetonitrile most likely corresponds to reduction of $(CH_3CN)SiMe_3^+$: M. Okano, K. Mocida, Chem. Lett. (1991) 819. As in our fragmentation process the O–Si bond cleavage will be assisted by concomitant bond formation of acetonitrile to the incipient silyl cation, the reduction potential of $(CH_3CN)SiMe_3^+$ is a reasonable approximation to evaluate the bond cleavage mode.
[32] E. Jungermann, J.J. McBride, Jr., R. Clutter, A. Mais, J. Org. Chem. 27 (1962) 606.
[33] (a) A.H. Cowley, R.A. Kemp, Chem. Rev. 85 (1985) 367;
(b) G. Boche, P. Andrews, K. Harms, M. Marsch, K.S. Rangaappa, M. Schimeczek, C. Willeke, J. Am. Chem. Soc. 118 (1996) 4925.
[34] A.G. Csaky, J. Plumet, Chem. Soc. Rev. 30 (2001) 313.
[35] Diketones: (a) E. Baciocchi, A. Casu, R. Ruzziconi, Tetrahedron Lett. 30 (1989) 3707;
(b) S.E. Drewes, C.J. Hogan, P.T. Kaye, G.H.P. Roos, J. Chem. Soc. Perkin Trans. 1 (1989) 1585;
(c) K.D. Moeller, L.V. Tinao, J. Am. Chem. Soc. 114 (1992) 1033;
(d) T. Fujii, T. Hirao, Y. Ohshiro, Tetrahedron Lett. 33 (1992) 5823;
(e) A.B. Paolobelli, D. Latini, R. Ruzziconi, Tetrahedron Lett. 34 (1993) 721;
(f) K. Ryter, T. Livinghouse, J. Am. Chem. Soc. 120 (1998) 2658.
[36] Dicarboxylic acids and derivatives: (a) J.H. Babler, S.J. Sarussi, J. Org. Chem. 52 (1987) 3462;
(b) P. Renaud, M.A. Fox, J. Org. Chem. 53 (1988) 3745;
(c) R. Peek, M. Streukens, H.G. Thomas, A. Vanderfuhr, U. Wellen, Chem. Ber. 127 (1994) 1257.
[37] For some special cases, cross-coupling of two different silyl enol ethers has been accomplished *via* intermediate radical cations using chemical one-electron oxidants. This approach, however, requires a very subtle control over the oxidation potentials of both reactants as well as their steric requirements, cf. Ref. 35a,e,f.
[38] (a) T. Langer, M. Illich, G. Helmchen, Synlett (1996) 1137;
(b) P.Q. Nguyen, H.J. Schäfer, Org. Lett. 3 (2001) 2993.
[39] (a) M. Schmittel, A. Burghart, W. Malisch, J. Reising, R. Söllner, J. Org. Chem. 63 (1998) 396;
(b) Z.A. Fataftah, M.R. Ibrahim, M.S. Abu-Agil, Tetrahedron Lett. 27 (1986) 4067.
[40] (a) M.W. Rathke, P.D. Weipert, Synth. Commun. 21 (1991) 1337;
(b) S.S. Washburne, W.R. Peterson, Jr., J. Organomet. Chem. 21 (1970) 59.
[41] (a) M.D. Curtis, S. Thanedar, W.M. Butler, Organometallics 3 (1984) 1855;
(b) P. Veya, C. Floriani, A. Chiesi-Villa, C. Rizzoli, Organometallics 12 (1993) 4892.
[42] G. Bringmann, S. Tasler, Tetrahedron 57 (2001) 331 (and literature therein).
[43] (a) A. Haeuseler, PhD thesis Siegen, 2001.;
(b) M. Schmittel, A. Haeuseler, publication in preparation.